

Research Article

Wide-Gap $p\text{-}\mu\text{c-Si}_{1-x}\text{O}_x\text{:H}$ Films and Their Application to Amorphous Silicon Solar Cells

Taweewat Krajangsang, Sorapong Inthisang, Aswin Hongsingthong, Amornrat Limmanee, Jaran Sritharathikhun, and Kobsak Sriprapha

Solar Energy Technology Laboratory, National Electronics and Computer Technology Center, National Science and Technology Development Agency, 112 Thailand Science Park, Phahonyothin Road, Klong 1, Klong Luang, Pathumthani 12120, Thailand

Correspondence should be addressed to Taweewat Krajangsang; taweewat.krajangsang@nectec.or.th

Received 1 February 2013; Revised 6 June 2013; Accepted 1 July 2013

Academic Editor: Junsin Yi

Copyright © 2013 Taweewat Krajangsang et al. This is an open access article distributed under the Creative Commons Attribution License, which permits unrestricted use, distribution, and reproduction in any medium, provided the original work is properly cited.

Optimization of p-type hydrogenated microcrystalline silicon oxide thin films ($p\text{-}\mu\text{c-Si}_{1-x}\text{O}_x\text{:H}$) by very high frequency plasma enhanced chemical vapor deposition 40 MHz method for use as a p-layer of a-Si:H solar cells was performed. The properties of $p\text{-}\mu\text{c-Si}_{1-x}\text{O}_x\text{:H}$ films were characterized by conductivity, Raman scattering spectroscopy, and spectroscopic ellipsometry. The wide optical band gap $p\text{-}\mu\text{c-Si}_{1-x}\text{O}_x\text{:H}$ films were optimized by CO_2/SiH_4 ratio and H_2/SiH_4 dilution. Besides, the effects of wide-gap $p\text{-}\mu\text{c-Si}_{1-x}\text{O}_x\text{:H}$ layer on the performance of a-Si:H solar cells with various optical band gaps of p-layer were also investigated. Furthermore, improvements of open circuit voltage, short circuit current, and performance of the solar cells by using the effective wide-gap $p\text{-}\mu\text{c-Si}_{1-x}\text{O}_x\text{:H}$ were observed in this study. These results indicate that wide-gap $p\text{-}\mu\text{c-Si}_{1-x}\text{O}_x\text{:H}$ is promising to use as window layer in a-Si:H solar cells.

1. Introduction

At present, solar cell technologies are becoming one of the most promising clean energies. For commercial use, solar cell modules can be divided into wafer based crystalline silicon (c-Si) and thin films. In the case of thin film, solar cell technologies are cadmium telluride (CdTe), copper indium gallium (di) selenide (CIGS), and amorphous silicon (a-Si:H). The multijunction silicon-based thin film solar cells are attractive candidates for further low-cost and highly efficient solar cells. The development of thin film silicon solar cells which were suitable to use in tropical climate region has been reported by our group [1–3]. Therefore, the optimization of single-junction a-Si:H solar cells is necessary to obtain higher efficiency in amorphous silicon oxide/amorphous silicon (a-SiO:H/a-Si:H) or in amorphous silicon/microcrystalline silicon (a-Si:H/ $\mu\text{c-Si:H}$) tandem cells. Several reports demonstrated that a heterojunction p/i interface was important to achieve high efficiency in a-Si:H and $\mu\text{c-Si:H}$ solar cells [4–6]. Normally, the hydrogenated amorphous silicon carbide (a-SiC:H) and amorphous silicon oxide (a-SiO:H) films were

used in the p-layer as wide band gap material [7–11]. Meanwhile, the wide optical band gap hydrogenated microcrystalline silicon oxide p-type ($p\text{-}\mu\text{c-Si}_{1-x}\text{O}_x\text{:H}$), which could be a mixture of SiO microcrystallites and Si microcrystallites, a mixture of amorphous SiO and Si microcrystallites, or a mixture of amorphous SiO and SiO microcrystallites, was promising material for use as the p-layer in p-i-n structure silicon-based solar cells due to the low absorption coefficient and high conductivity. The oxygen-rich phase was effective in increasing the optical band gap and the silicon-rich phase contributed to high conductivity [12, 13]. In our previous work, we studied the effect of p-layer band gap on the performance of $\mu\text{c-Si:H}$ p-i-n type single-junction solar cells by theoretical and experimental analysis [6]. The advantage of the $p\text{-}\mu\text{c-Si}_{1-x}\text{O}_x\text{:H}$ film compared with $p\text{-}\mu\text{c-Si:H}$ film is a wide optical band gap (E_{04}), which is effective in the enhancement of light absorption and has built-in potential in i-layer. The strong built-in potential could reduce the recombination between p-i interface and in the bulk material [14]. Therefore, photovoltaic parameters could be improved, resulting in the increase of solar cell efficiency. However,

TABLE 1: Deposition condition for p- μ c-Si_{1-x}O_x:H films.

| Parameters | Values |
|-----------------------|-----------------------|
| Gas flow | |
| SiH ₄ | 2.4 sccm |
| H ₂ | 200–360 sccm |
| TMB (3%) | 1.2 sccm |
| CO ₂ | 0–1.2 sccm |
| Power density | 83 mW/cm ² |
| Deposition pressure | 500 mTorr |
| Substrate temperature | 180°C |

it was found that the conductivity of the p- μ c-Si_{1-x}O_x:H film seems to be lower than that of the p- μ c-Si:H at the same optical band gap. In order to obtain solar cells with high conversion efficiency, it is necessary to improve p- μ c-Si_{1-x}O_x:H with high conductivity and wide optical band gap.

In this paper, we present our experimental study to improve the properties of wide optical band gap p- μ c-Si_{1-x}O_x:H films and investigate the effect of wide-gap p- μ c-Si_{1-x}O_x:H layer on the performance of a-Si:H solar cells.

2. Experimental Details

2.1. Preparation of p- μ c-Si_{1-x}O_x:H Films. Firstly, the optimization of p- μ c-Si:H and p- μ c-Si_{1-x}O_x:H films was performed. The p- μ c-Si:H and p- μ c-Si_{1-x}O_x:H films were deposited on Soda-lime glass substrates by 40 MHz very high frequency plasma enhanced chemical vapor deposition (VHF-PECVD) in a multichamber with a parallel plate configuration. We used silane (SiH₄), hydrogen (H₂), and carbon dioxide (CO₂) as reactant gases and 3%-hydrogen-diluted trimethylboron (TMB: B(CH₃)₃) as a doping gas. The temperature, pressure, and power density for deposition were kept at 180°C, 500 mTorr and 83 mW/cm², respectively. The deposition conditions are summarized in Table 1. After that, effects of CO₂/SiH₄ ratio and H₂/SiH₄ dilution on the film properties were investigated.

The dark conductivity (σ_d) and activation energy (E_a) were measured with Al coplanar electrode configuration. Spectroscopic ellipsometry was used to determine the optical properties and thickness of these films. The measurement data were fit and analyzed using the Tauc-Lorentz model [15]. The Fourier transform infrared spectroscopy (FTIR) absorption measurement was used to estimate the concentration of oxygen (C[O] at.%) and hydrogen (C[H] at.%) within the film measurements on polished monocrystalline high-resistance silicon wafer samples [16]. The structural properties of the films were characterized by Raman scattering spectroscopy. The crystalline volume fraction (X_c) was calculated from $X_c = (I_{510} + I_{520}) / (I_{480} + I_{510} + I_{520})$, where I_{520} , I_{510} , and I_{480} were integrated intensities corresponding to the crystalline, intermediate, and amorphous phase in the material, respectively [17, 18].

2.2. Fabrication of a-Si:H Solar Cells. The a-Si:H solar cells with p- μ c-Si:H and p- μ c-Si_{1-x}O_x:H window layer were

fabricated. The intrinsic hydrogenated amorphous silicon (i-a-Si:H) was prepared by 60 MHz VHF-PECVD and output power density was kept constant at 37.5 mW/cm². The pressure deposition of i-layer was kept at 500 mTorr. The dark conductivity and optical band gap (E_{opt}) of i-a-Si:H film were 2.02×10^{-9} S/cm and 1.80 eV, respectively. The μ c-Si:H n-layer was doped by 3%-hydrogen-diluted phosphine (PH₃) and prepared by 60 MHz VHF-PECVD with a power density of 66 mW/cm². The dark conductivity, activation energy, and optical band gap (E_{04}) of μ c-Si:H film was 5.3 S/cm, 0.05 eV, and 2.10 eV, respectively. The fabrication temperature of a-Si:H solar cells was kept at 200°C. The a-Si:H solar cells had a structure of glass/SnO₂/ZnO:Al/p- μ c-Si_{1-x}O_x:H (35 nm)/i-a-Si:H (400 nm)/n- μ c-Si:H (35 nm)/ZnO:Al/Ag. The active area of the solar cells was divided by laser scribing into 1 cm². The photovoltaic parameters of the solar cells have been investigated under standard conditions (AM 1.5, 100 mW/cm², and 25°C) with a double light source solar simulator. The quantum efficiency (QE) of the solar cells has been characterized by spectral response measurements.

3. Results and Discussions

3.1. Effects of CO₂/SiH₄ Ratio. The effects of CO₂/SiH₄ ratio on the optical and electrical properties of p- μ c-Si_{1-x}O_x:H films were investigated. The CO₂ was used as the source gas for O atom in the deposition of the p- μ c-Si_{1-x}O_x:H film. The samples were prepared by increasing CO₂/SiH₄ ratio from 0 to 1.2 with the thickness of about 100 nm as well as by keeping H₂/SiH₄ and TMB/SiH₄ at 116 and 1.5, respectively. Figure 1 shows the dependence of the dark conductivity and activation energy on the CO₂/SiH₄ ratio for p- μ c-Si_{1-x}O_x:H films. By increasing the CO₂/SiH₄ ratio from 0.0 to 0.5, the dark conductivity decreased from 2.66×10^{-1} S/cm to 2.17×10^{-4} S/cm, while the activation energy increased from 0.05 eV to 0.28 eV. In this study, the band gap of p-layer was calculated from the optical band gap. E_{04} , the photon energy which corresponds to absorption coefficient of 10^4 cm⁻¹, was used to define the band gap of p-layer. For comparison, absorption spectra of p- μ c-Si:H and p- μ c-Si_{1-x}O_x:H measured by Spectroscopic ellipsometry are shown in Figure 2. It can be seen that in the case of p- μ c-Si_{1-x}O_x:H film, the optical absorption edge is shifted towards higher photon energy compared to conventional p-c-Si:H film. With increasing CO₂/SiH₄ ratio, the optical band gap (E_{04}) increased from 2.08 eV to 2.18 eV. The optical band gap became wider because of increased Si-O bonds in amorphous silicon oxide (a-SiO) phase [5, 6]. To clarify this result, the FTIR measurement was performed. Figure 3 shows infrared absorption spectra of p- μ c-Si_{1-x}O_x:H films as a function of CO₂/SiH₄ ratio with oxygen and hydrogen concentration. The increasing of CO₂/SiH₄ ratio was not only to increase the oxygen concentration, but also to increase the hydrogen concentration. As result, with CO₂/SiH₄ ratio of 0.0 to 0.5, the oxygen and hydrogen concentration were increased from 0.5 at.% to 14.5 at.% and 9.3 at.% to 28.3 at.%, respectively. From this result, it is clearly seen that the increase of CO₂/SiH₄ ratio played

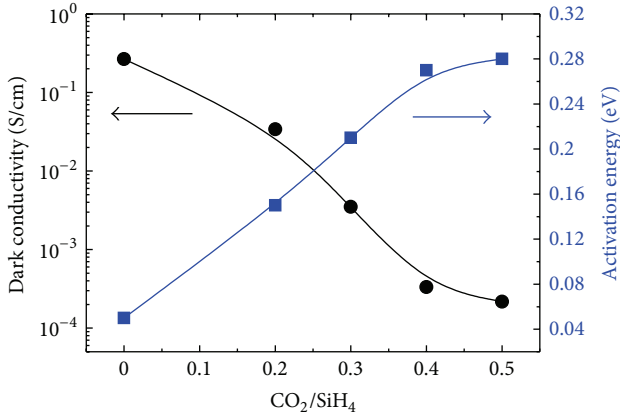


FIGURE 1: Dependence of the dark conductivity and activation energy on the CO₂/SiH₄ ratio for p-μc-Si_{1-x}O_x:H films.

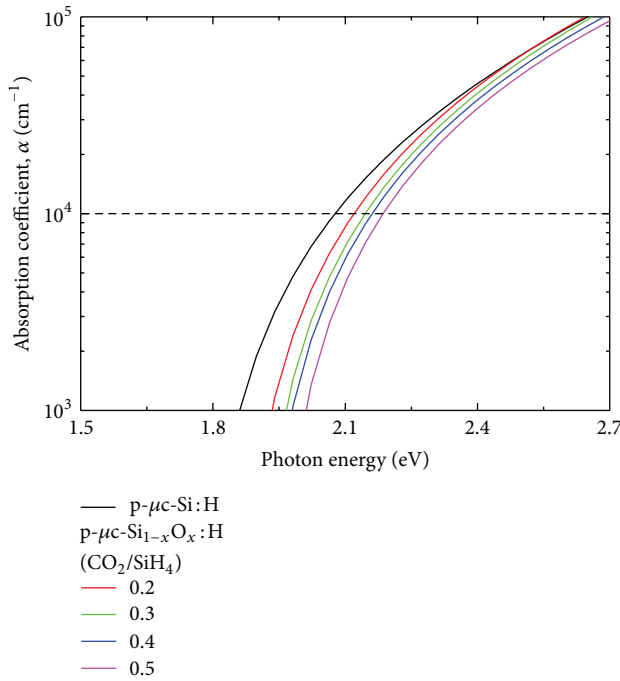


FIGURE 2: Dependence of the absorption coefficient on the CO₂/SiH₄ ratio for p-μc-Si_{1-x}O_x:H films.

the role to improve the optical band gap of the p-μc-Si_{1-x}O_x:H films. However, this method leads to the deterioration of the electrical property of the films which may be due to the increase of dangling bond and microcrystalline phase; this was prevented during the deposition process. Figure 4 shows dependence of the crystalline volume fraction of p-μc-Si_{1-x}O_x:H films on the CO₂/SiH₄ ratio. The crystalline volume fraction decreased from 49% to 4% as the CO₂/SiH₄ ratio increased. From these results, it was clear that there was a tradeoff between optical and electrical properties as well as film structure when the oxygen atoms participate in the films. Therefore, p-μc-Si_{1-x}O_x:H films should be further optimized.

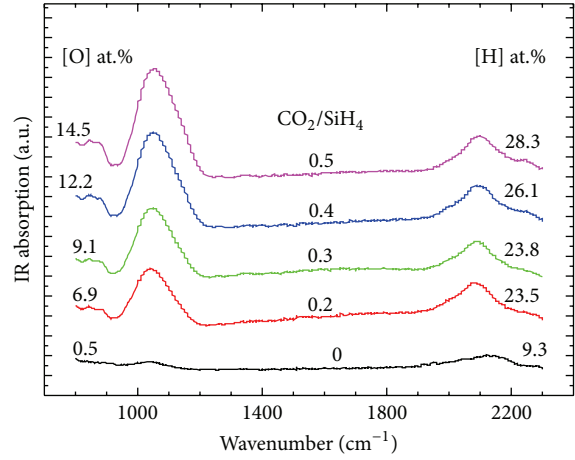


FIGURE 3: Infrared absorption spectra of p-μc-Si_{1-x}O_x:H films as a function of CO₂/SiH₄ ratio with oxygen and hydrogen concentration.

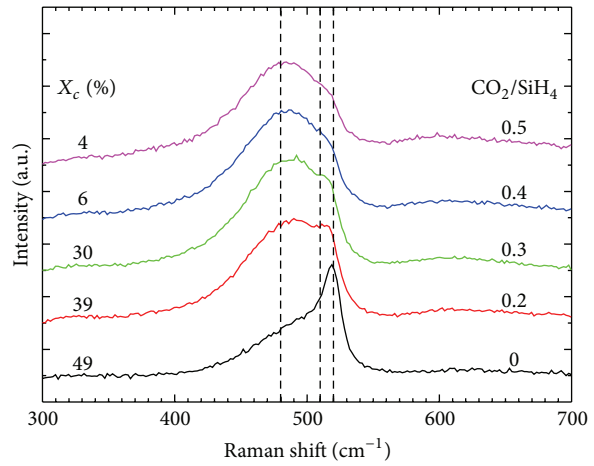


FIGURE 4: Dependence of the crystalline volume fraction on the CO₂/SiH₄ ratio for p-μc-Si_{1-x}O_x:H films.

3.2. Effects of H₂/SiH₄ Dilution. To further improve the properties of p-μc-Si_{1-x}O_x:H film, the effects of H₂/SiH₄ dilution on the optical and electrical properties of p-μc-Si_{1-x}O_x:H film were studied. The H₂/SiH₄ dilution was varied from 83 to 150. The CO₂/SiH₄ dilution and TMB/SiH₄ were kept at 0.2 and 1.5, respectively. Figure 5 shows the dependence of the dark conductivity and activation energy on the H₂/SiH₄ dilution. The dark conductivity increased from 5.35 × 10⁻⁷ S/cm to 2.33 × 10⁻² S/cm while the activation energy decreased from 0.3 to 0.07 eV as the H₂/SiH₄ dilution increased. Besides, the absorption spectra of these films were not clearly changed in the optical band gap as shown in Figure 6. Figure 7 shows the FTIR results of p-μc-Si_{1-x}O_x:H films deposited with various H₂/SiH₄ dilution. In viewing this graph, it can be seen that the oxygen concentration slightly changed between 5.7 at.% and 6.6 at.%; meanwhile the hydrogen concentration was decreased from 20.3 at.% to 18.5 at.% with increasing H₂/SiH₄ dilution from 83 to 100. Hydrogen concentration first increased from 18.5 at.% to

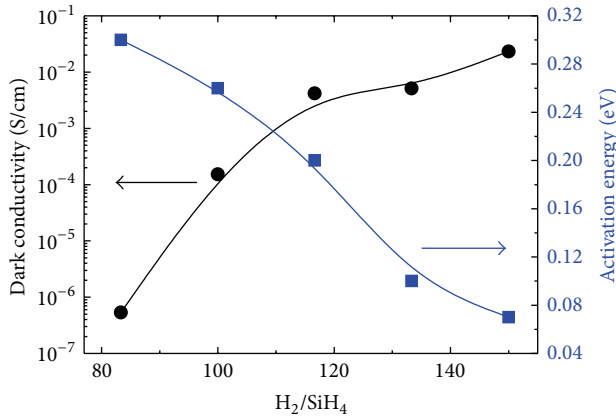
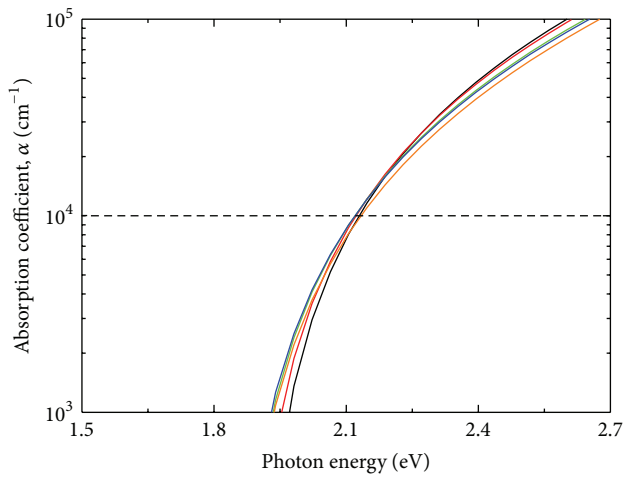


FIGURE 5: Dependence of the dark conductivity and activation energy on the H_2/SiH_4 dilution for $p-\mu c-Si_{1-x}O_x:H$ films.



$p-\mu c-Si_{1-x}O_x:H$
 H_2/SiH_4
 — 83
 — 100
 — 117
 — 133
 — 150

FIGURE 6: Dependence of the absorption coefficient on the H_2/SiH_4 ratio for $p-\mu c-Si_{1-x}O_x:H$ films.

26.0 at.% in the phase transition region and then decreased to 21.3 at.% when films changed to the microcrystalline mixed phase as can be seen from Raman spectral in Figure 8. Figure 8 shows dependence of the crystalline volume fraction of $p-Si_{1-x}O_x:H$ films on the H_2/SiH_4 dilution. The crystalline volume fraction increased from 0% to 43% as the H_2/SiH_4 dilution increased.

In this work, the optimum condition for $p-\mu c-Si_{1-x}O_x:H$ film was obtained at CO_2/SiH_4 ratio and H_2/SiH_4 dilution of 0.2 and 150, respectively. By using this optimum condition, excellent film properties were achieved with the wide optical band gap of 2.13 eV. The dark conductivity and crystalline

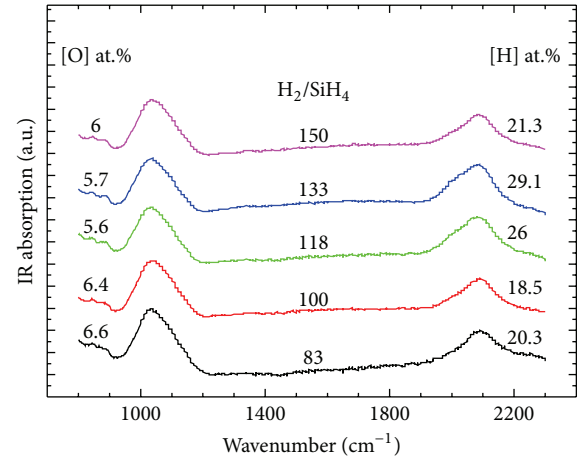


FIGURE 7: Infrared absorption spectra of $p-\mu c-Si_{1-x}O_x:H$ films as a function of H_2/SiH_4 ratio with oxygen and hydrogen concentration.

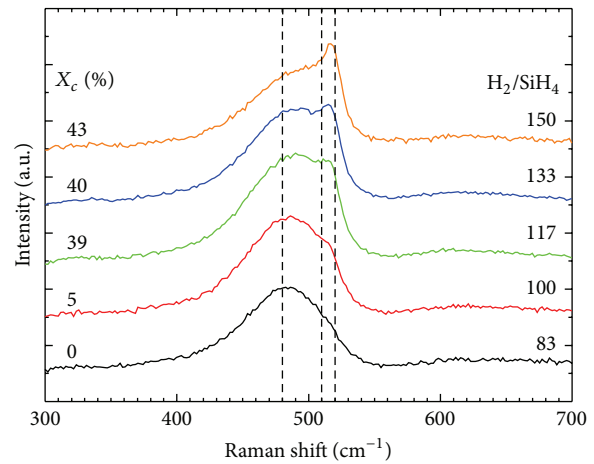


FIGURE 8: Dependence of the crystalline volume fraction on the H_2/SiH_4 dilution for $p-\mu c-Si_{1-x}O_x:H$ films.

volume fraction of the optimized film were 2.33×10^{-2} S/cm and 43%, respectively.

3.3. Effect of p-layer Optical Band Gap on Performance of a-Si:H Solar Cells. In order to investigate how the optical band gap of p-layer influences the performance of a-Si:H solar cells, the effect of p-layer with various optical band gap was then studied. Figure 9 shows typical photo $I-V$ characteristics of a-Si:H solar cells using $p-\mu c-Si_{1-x}O_x:H$ p-layer with the optical band gap 2.28 eV, 2.22 eV, and p-c-Si:H p-layer with the optical band gap 2.09 eV. The open circuit voltage (V_{oc}) was increased from 0.87 V to 0.91 V with an increasing optical band gap of p-layer and solar cells; efficiency was increased from 8.8% to 9.7%. The photovoltaic parameters are summarized in Table 2. Figure 10 shows the quantum efficiencies of a-Si:H solar cells with various p-layer band gap. The spectral response of a-Si:H solar cells was increased with increasing optical band gap of p-layer which corresponds to an increase in the short circuit current (J_{sc}).

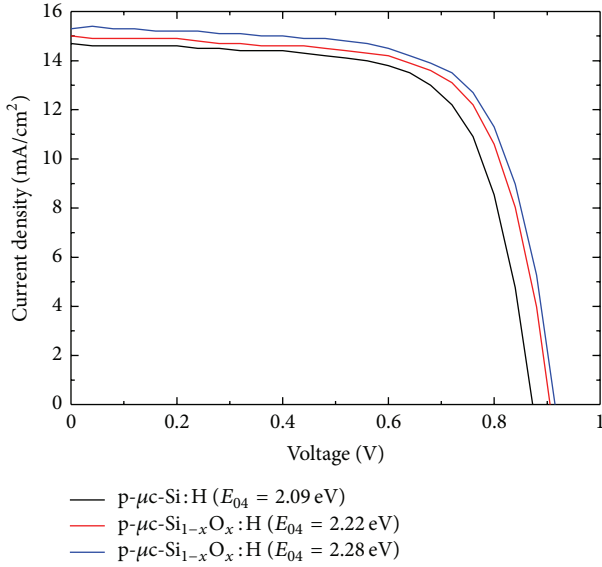


FIGURE 9: I - V characteristics of a-Si:H solar cells with p- μ c-Si:H and p- μ c-Si $_{1-x}$ O $_x$:H layers.

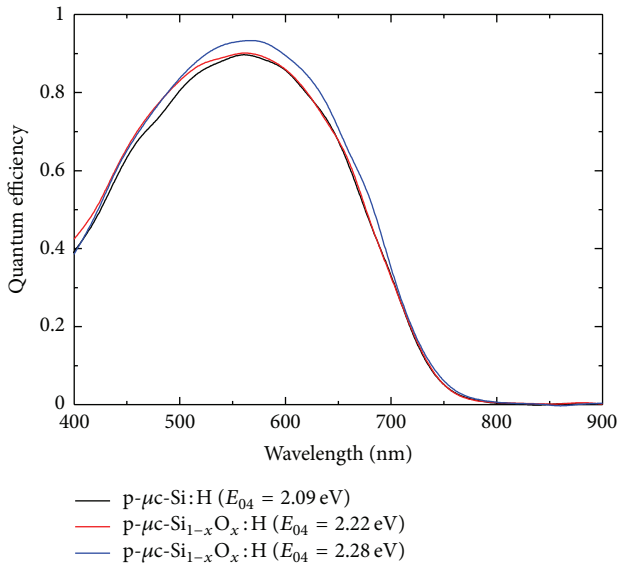


FIGURE 10: Quantum efficiencies of a-Si:H solar cells with p- μ c-Si:H and p- μ c-Si $_{1-x}$ O $_x$:H layers.

The improvement of the J_{sc} might be due to low absorption coefficients of the wide-gap p-layer that led to an increase in light which goes to i-layer. On the other hand, the spectral responses in short wavelength region at lower than 450 nm were not clearly different. This might be due to absorption of SnO $_2$ and ZnO:Al front transparent conductive oxide. The results showed that the band gap of p-layer influenced the V_{oc} of a-Si:H solar cell. The increase of V_{oc} by using wide band gap p-layer was observed because the potential barrier at p/i interface increases which suppresses the electron backdiffusion from i-layer to p-layer. The suppression of the back diffusion results in the low recombination in the p-layer

TABLE 2: Photovoltaic characteristics of a-Si:H solar cells using p-layer with various optical band gaps.

| p-layer band gap, E_{04} (eV) | V_{oc} (V) | J_{sc} (mA/cm 2) | FF | Eff (%) |
|---------------------------------|--------------|------------------------|------|---------|
| 2.09 | 0.87 | 14.7 | 0.69 | 8.8 |
| 2.22 | 0.90 | 15.0 | 0.70 | 9.4 |
| 2.28 | 0.91 | 15.4 | 0.69 | 9.7 |

or at the p/i interface. Therefore, it is clear that wide-gap p-c-Si $_{1-x}$ O $_x$:H film is beneficial to improve the performance of a-Si:H solar cells.

4. Conclusion

The p- μ c-Si $_{1-x}$ O $_x$:H films was optimized for application in the a-Si:H solar cells. We also investigated effects of wide-gap p- μ c-Si $_{1-x}$ O $_x$:H layer on the solar cell performance as described in this study. The optical band gap and electrical properties of p- μ c-Si $_{1-x}$ O $_x$:H films by an optimized condition of CO $_2$ /SiH $_4$ ratio and H $_2$ /SiH $_4$ dilution were obviously improved. Interestingly, the increase of V_{oc} and efficiency of the a-Si:H solar cells by using effective wide-gap μ c-Si $_{1-x}$ O $_x$:H p-layer were demonstrated. It is clear that wide-gap p- μ c-Si $_{1-x}$ O $_x$:H film can improve the performance of a-Si:H solar cells.

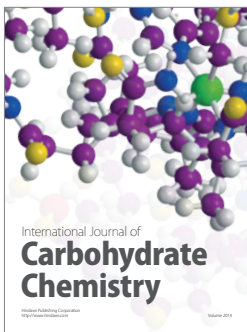
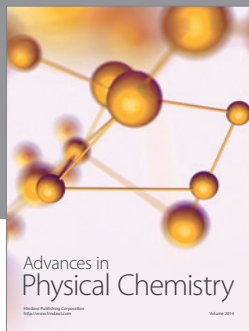
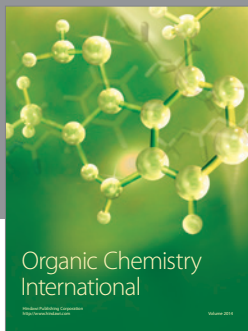
Acknowledgment

This work was financially supported by Cluster and Program Management Office (CPM) of NSTDA, Thailand.

References

- [1] K. Sriprapha, I. A. Yunaz, S. Hiza et al., "Temperature dependence of silicon-based thin film solar cells on their intrinsic absorber," *MRS Proceedings*, vol. 989, 2007.
- [2] K. Sriprapha, S. Inthisang, S. Y. Myong et al., "Development of amorphous silicon-based thin-film solar cells with low-temperature coefficient," in *Proceedings of SPIE 7045, Photovoltaic Cell and Module Technologies II*, August 2008.
- [3] K. Sriprapha, S. Y. Myong, A. Yamada, and M. Konagai, "Temperature dependence of protocrystalline silicon/microcrystalline silicon double-junction solar cells," *Japanese Journal of Applied Physics*, vol. 47, no. 3, pp. 1496–1500, 2008.
- [4] K. Chikusa, K. Takemoto, T. Itoh, N. Yoshida, and S. Nonomura, "Preparation of B-doped a-Si $_{1-x}$ C $_x$:H films and heterojunction p-i-n solar cells by the Cat-CVD method," *Thin Solid Films*, vol. 430, no. 1-2, pp. 245–248, 2003.
- [5] S. Miyajima, A. Yamada, and M. Konagai, "Highly conductive microcrystalline silicon carbide films deposited by the hot wire cell method and its application to amorphous silicon solar cells," *Thin Solid Films*, vol. 430, no. 1-2, pp. 274–277, 2003.
- [6] T. Krajangsang, S. Kasashima, A. Hongsingthong, P. Sichanugrist, and M. Konagai, "Effect of p- μ c-Si $_{1-x}$ O $_x$:H layer on performance of hetero-junction microcrystalline silicon solar cells under light concentration," *Current Applied Physics*, vol. 12, no. 2, pp. 515–520, 2012.

- [7] S. Y. Myong, S. S. Kim, and K. S. Lim, "Improvement of pin-type amorphous silicon solar cell performance by employing double silicon-carbide p-layer structure," *Journal of Applied Physics*, vol. 95, no. 3, pp. 1525–1530, 2004.
- [8] S. Y. Myong, K. S. Lim, and J. M. Pears, "Double amorphous silicon-carbide p-layer structures producing highly stabilized pin-type polycrystalline silicon multilayer solar cells," *Applied Physics Letters*, vol. 87, no. 19, Article ID 193509, pp. 1–3, 2005.
- [9] M. I. Kabir, S. A. Shahahmadi, V. Lim, S. Zaidi, K. Sopian, and N. Amin, "Amorphous silicon single-junction thin-film solar cell exceeding 10% efficiency by design optimization," *International Journal of Photoenergy*, vol. 2012, Article ID 460919, p. 7, 2012.
- [10] Y. Matsumoto, F. Meléndez, and R. Asomoza, "Performance of p-type silicon-oxide windows in amorphous silicon solar cell," *Solar Energy Materials and Solar Cells*, vol. 66, no. 1–4, pp. 163–170, 2001.
- [11] K. Barua, A. Sarker, A. K. Bandyopadhyay, D. Das, and S. Ray, "Improvement in the conversion efficiency of single and double junction a-Si solar cells by using high quality p-SiO:H window layer and seed layer/thin n- μ c-Si:H layer," in *Proceedings of the IEEE 20th Photovoltaic Specialists Conference*, pp. 829–8832, 2000.
- [12] H. Watanabe, K. Haga, and T. Lohner, "Structure of high-photosensitivity silicon-oxygen alloy films," *Journal of Non-Crystalline Solids*, vol. 164–166, no. 2, pp. 1085–1088, 1993.
- [13] P. Sihanugrist, T. Sasaki, A. Asano, Y. Ichikawa, and H. Sakai, "Amorphous silicon oxide and its application to metal/n-i-p/ITO type a-Si solar cells," *Solar Energy Materials and Solar Cells*, vol. 34, no. 1–4, pp. 415–422, 1994.
- [14] W. Luft and Y. S. Tsuo, *Hydrogenated Amorphous Silicon Alloy Deposition Processes*, Marcel Dekker, New York, NY, USA, 1993.
- [15] H. Fujiwara, *Spectroscopic Ellipsometry: Principles and Application*, John Wiley & Sons, Chichester, UK, 2007.
- [16] G. Lucovsky, J. Yang, S. S. Chao, J. E. Tyler, and W. Czubytyj, "Oxygen-bonding environments in glow-discharge-deposited amorphous silicon-hydrogen alloy films," *Physical Review B*, vol. 28, no. 6, pp. 3225–3233, 1983.
- [17] I. H. Campbell and P. M. Fauchet, "The effects of microcrystal size and shape on the one phonon Raman spectra of crystalline semiconductors," *Solid State Communications*, vol. 58, no. 10, pp. 739–741, 1986.
- [18] T. Kaneko, M. Wakagi, K.-I. Onisawa, and T. Minemura, "Change in crystalline morphologies of polycrystalline silicon films prepared by radio-frequency plasma-enhanced chemical vapor deposition using SiF₄+H₂ gas mixture at 350°C," *Applied Physics Letters*, vol. 64, no. 14, pp. 1865–1867, 1994.



Hindawi

Submit your manuscripts at
<http://www.hindawi.com>

